International Symposium on Cosmic Rays and Astrophysics (ISCRA-2017)

Features of energetic magnetospheric electron precipitation in the year of highest precipitation rates (1994)

G. A. Bazilevskaya[1], , M. S. Kalinin[1], M. B. Krainev[1], V. S. Makhmutov[1], Y. I. Stozhkov[1], A. K. Svirzhevskaya[1], N. S. Svirzhevsky[1], , and B. B. Gvozdevsky[2]

[1]Lebedev Physical Institute, Russian Academy of Sciences, Moscow, 119991 Russia

[2]Polar Geophysical Institute, Russian Academy of Sciences, Apatity, Murmansk region, 184209 Russia

MEPHI, Wednesday 21 June 2017

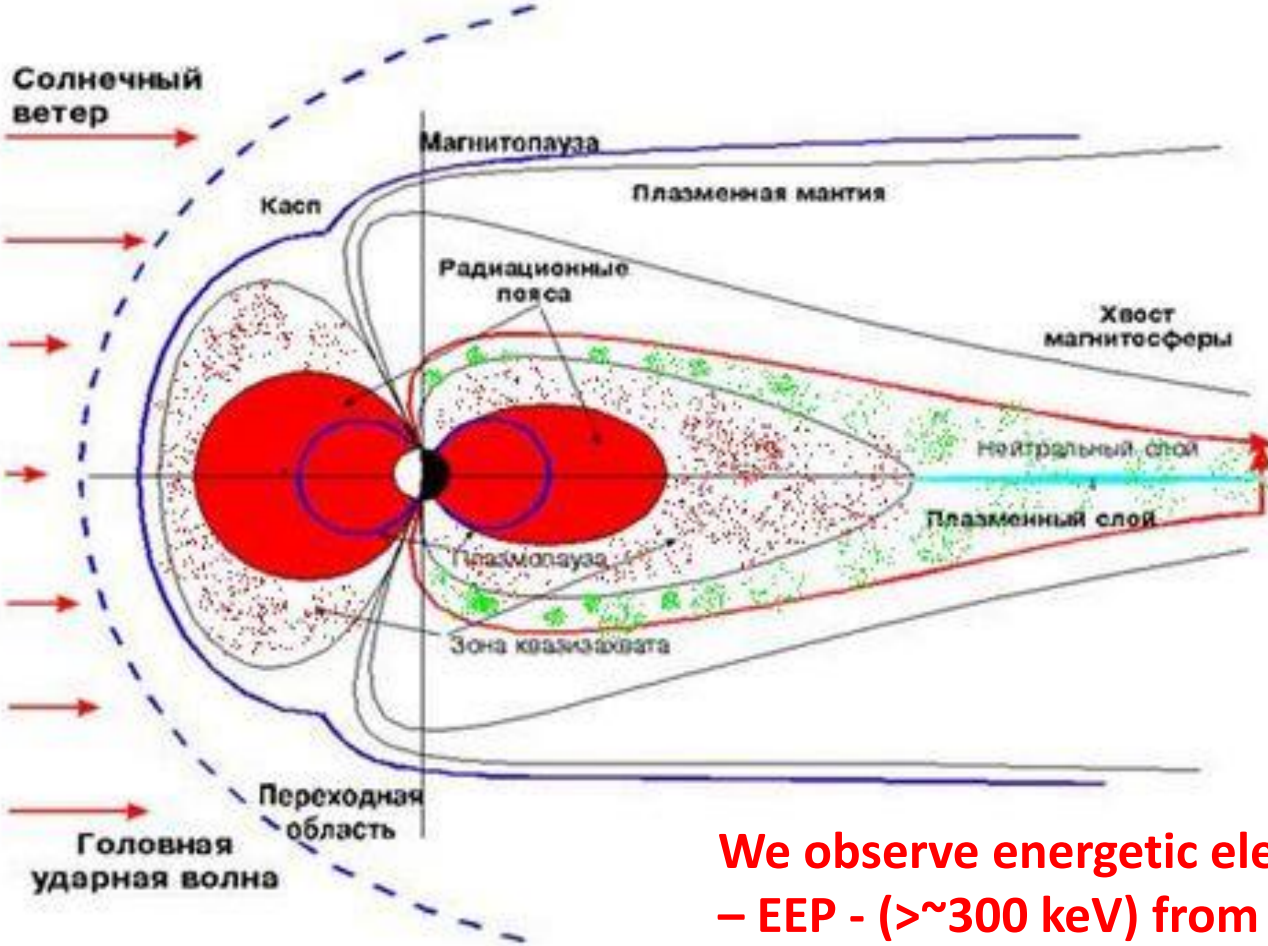

The classic picture of Earth's electron radiation belts exhibits a two-zone structure, with an inner belt peaking in intensity at radial distances less than ~2 Earth radii (RE) in Earth's magnetic equatorial plane and an outer belt peaking at radial distances between ~3 and ~6 RE, actually, 4.5 RE.
The outer zone extends from L ~ 2.5 at the inner edge to L ~ 6.5 at its outer edge.

We observe energetic electron precipitation – EEP - (>~300 keV) from the outer radiation belt.

Electrons are absorbed in the atmosphere at altitude >50 km. However, they generate X-rays via bremsstrahlung. Geiger counter is able to detect X-rays which penetrate down the altitudes ~20 km.

Significance of EEP for space weather

- **Satellite damage**

Deposit charge in insulators (e.g., cables) and circuit boards of satellites.

The most damaging electrons are believed to be those at a few MeV, and for this reason they have been termed "killer" electrons (Cumulative effects)

Change of the logic state of a device, and introduce errors into memory chips and other electronic devices, known as a single-event upset (SEU). (Horne, 2001)

- **Contribution to the ion-molecular reaction in the atmosphere: production of NOx and HOx and influence on the O_3**

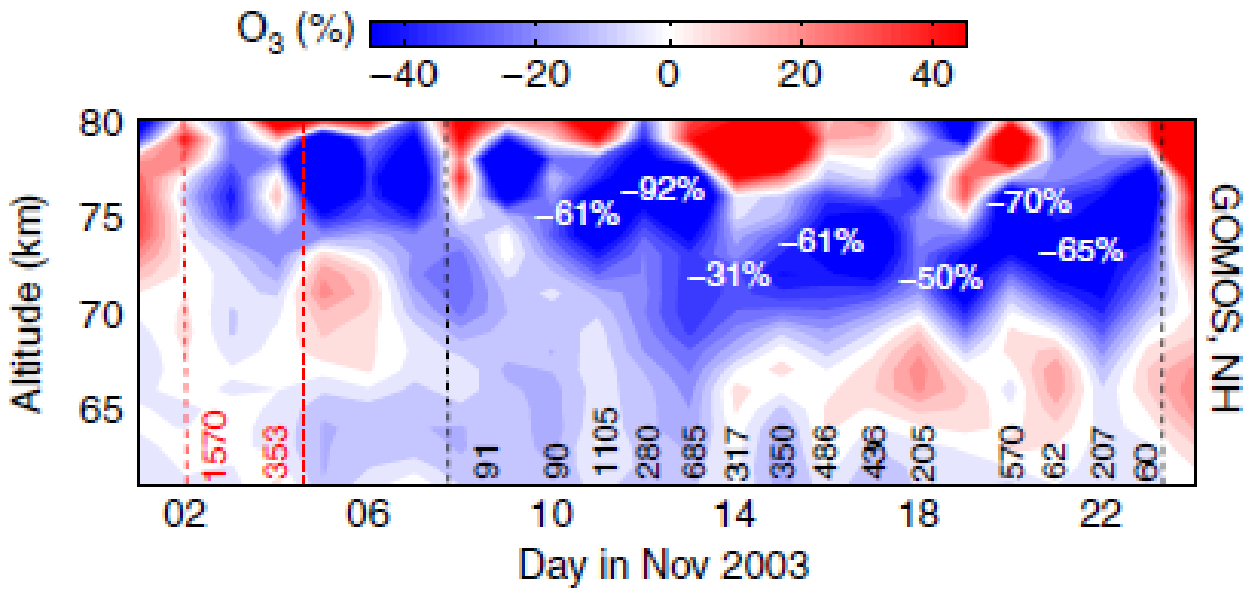

O_3 anomalies (%) for EEP events in the Northern hemisphere derived from GOMOS (Andersson, 2014), Black dashed lines: EEP event start and end; red dashed lines: SPE event start and end; black numbers: daily mean ECRs; red numbers: 410MeV pfu. White numbers: O_3 loss at different altitudes. The mesospheric ozone recovered from the effects of the SPE event by 7–8 November, before the strong EEP forcing is observed.

EEP – energetic electron precipitation, >~300 keV in our observations

A goal of the present work is to explain the EEP features as observed in the stratosphere in the frame of recent understanding of the acceleration and loss of energetic electrons of the outer radiation belt.

Outline

- Experiment description
- Energy transfer from interplanetary space to magnetospheric electrons
- EEP events in 1994. Are they in agreement with expected from recent ideas?
- Conclusion

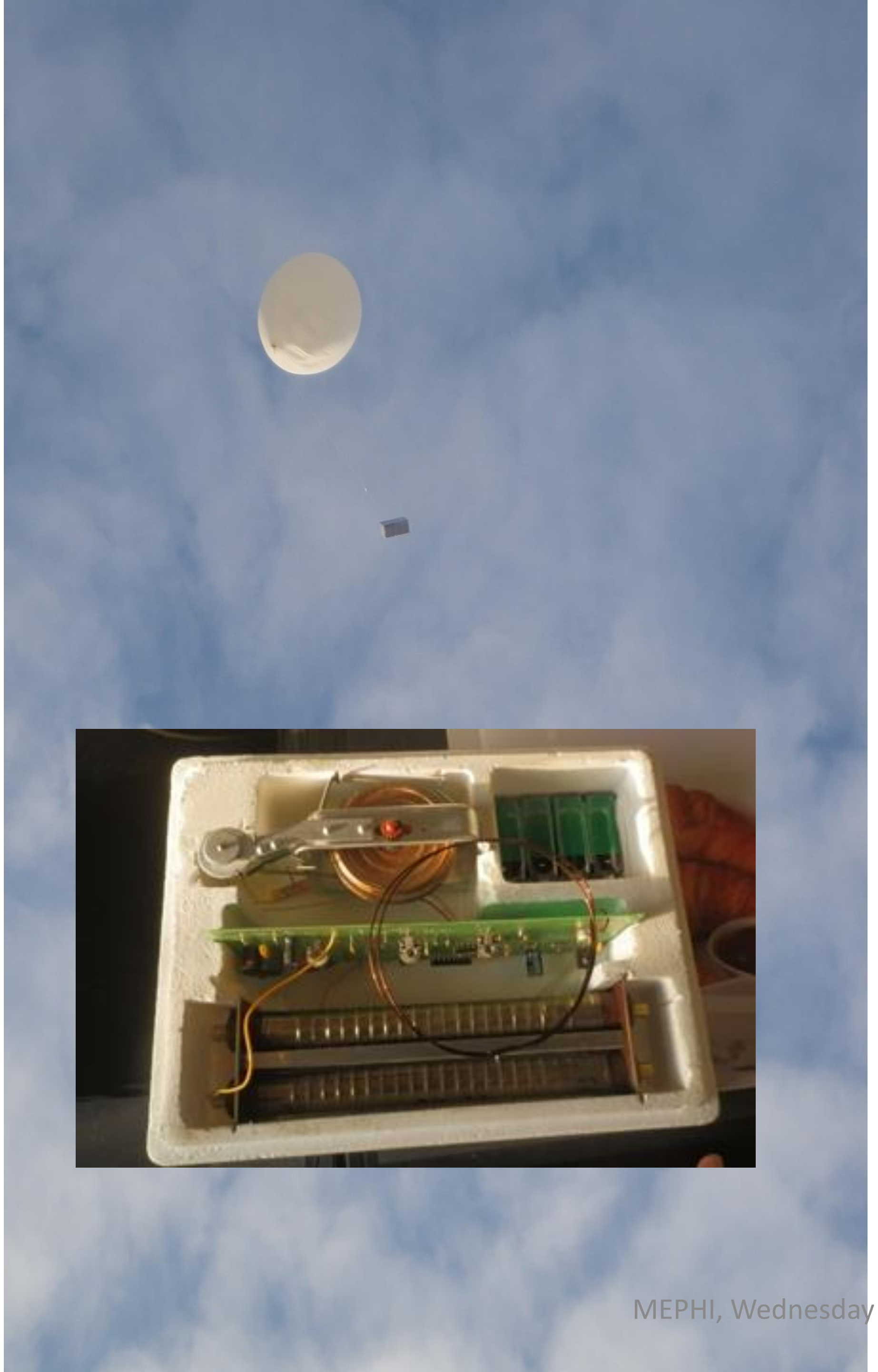

Several words about the long-term LPI cosmic ray experiment

- Measurement of charged particle fluxes at various levels of the atmosphere from ground level up to ~30-35 km and at several high and mid latitudes.
- Instrument: the Geiger counter telescope lifted on a meteorological balloon.
- Frequency of balloon launches and sites of observations before 1991 – every day, now 3 times a week, Murmansk and Moscow reg.,Antarctic
.

Detector thresholds and efficiency

Detector	Protons	Electrons	Muons	X-rays
Omni-directional counter	5 MeV (~100%)	200 keV (~100%)	1 MeV (~100%)	~1% (20-500 keV)
Telescope	30 MeV (~100%)	5 MeV (~100%)	15 MeV (~100%)	No

X-ray collides with a counter wall. A Compton electron ejected from an atom causes a discharge in the the counter

Charged particle fluxes in the Earth's atmosphere. Murmansk region

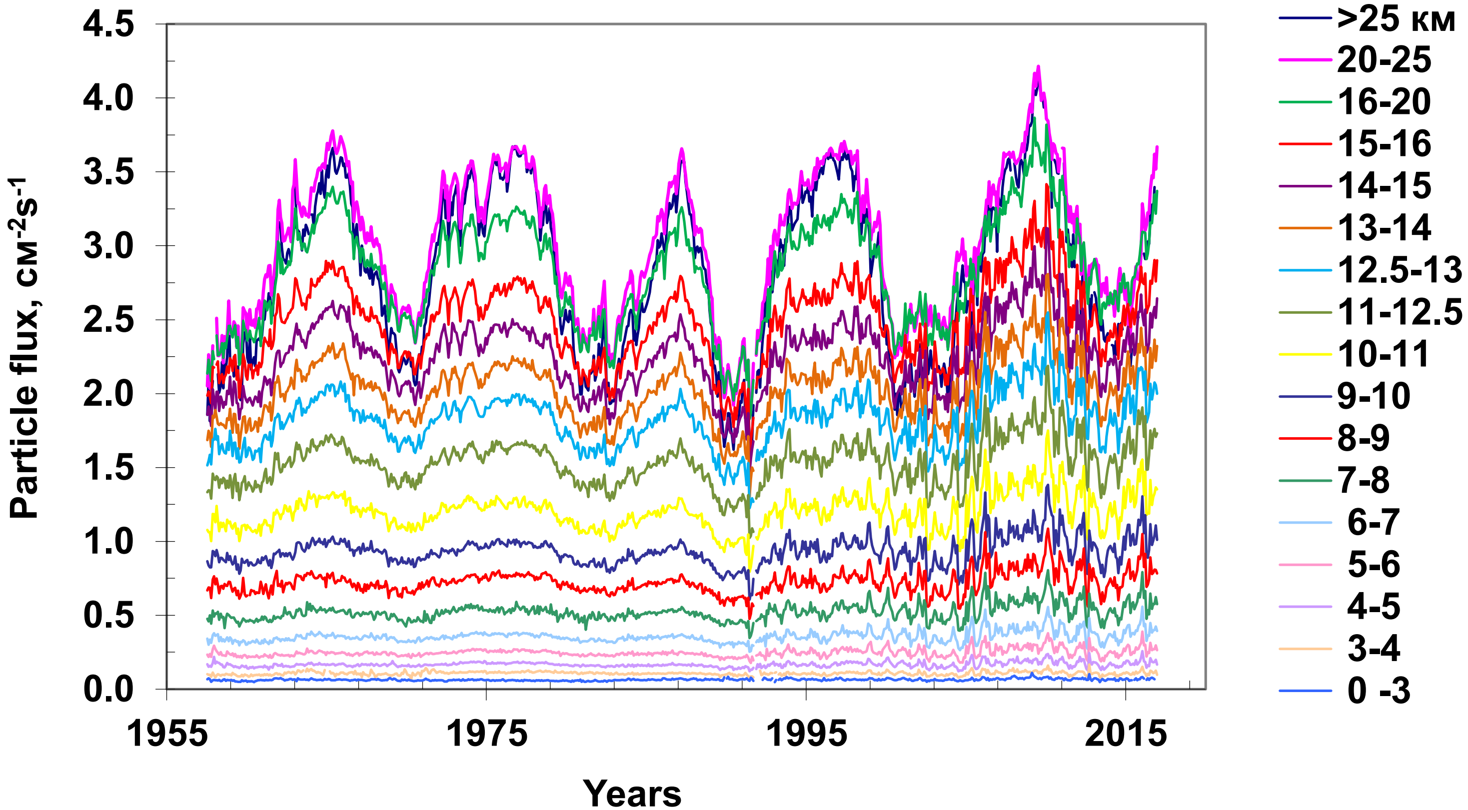

Stations

Launch location	Geographic/ Geomagnetic coordinates	Geomagn. Cutoff rigidity, GV	L-parameter	Period of observation	Time of EEP observation UT/MLT
Olenya station, Murmansk region	68°57'N/64.85 33°03'E/114.70	0,6	5.2-5.8	1957-2002	~08/ 10-11
Apatity, Murmansk region	67°33'N/63.94 33°20'E/112.85		5.2-5.3	2002 - наст. время	~10-14/ 13-17

Geomagnetic Locations of Stations

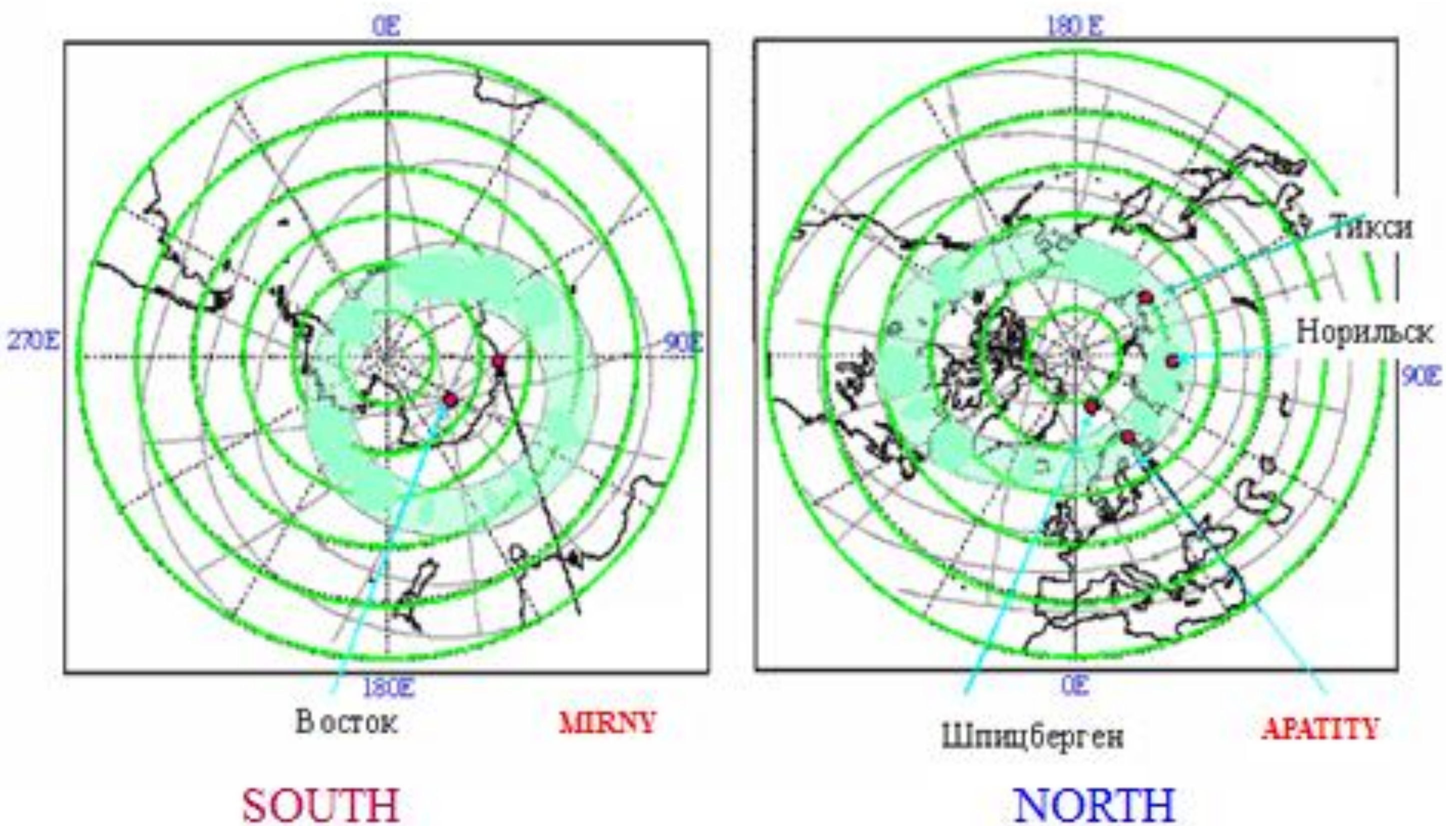

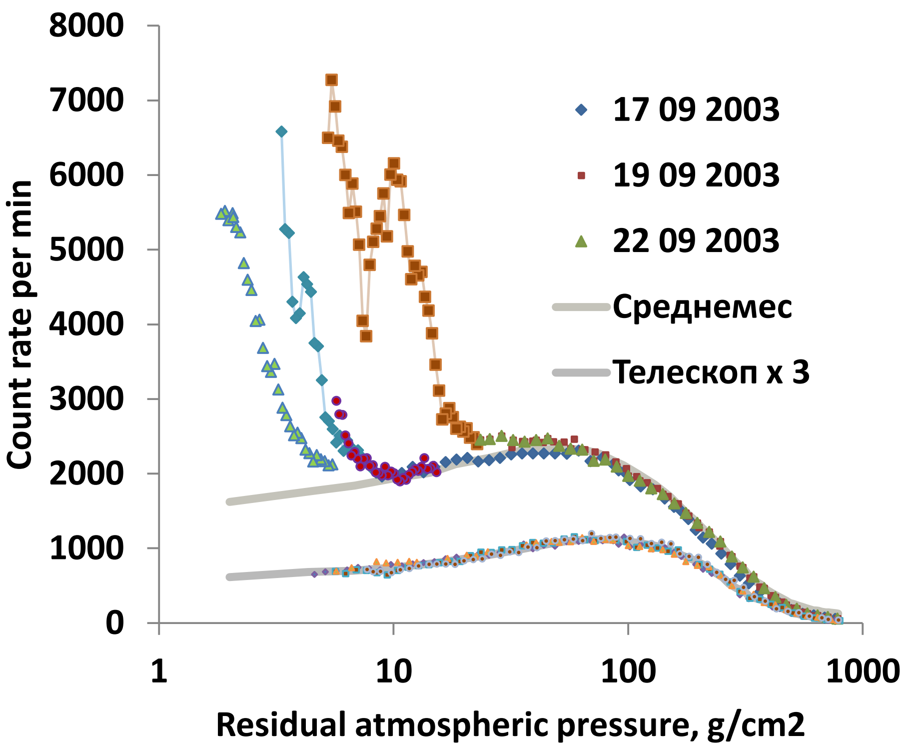

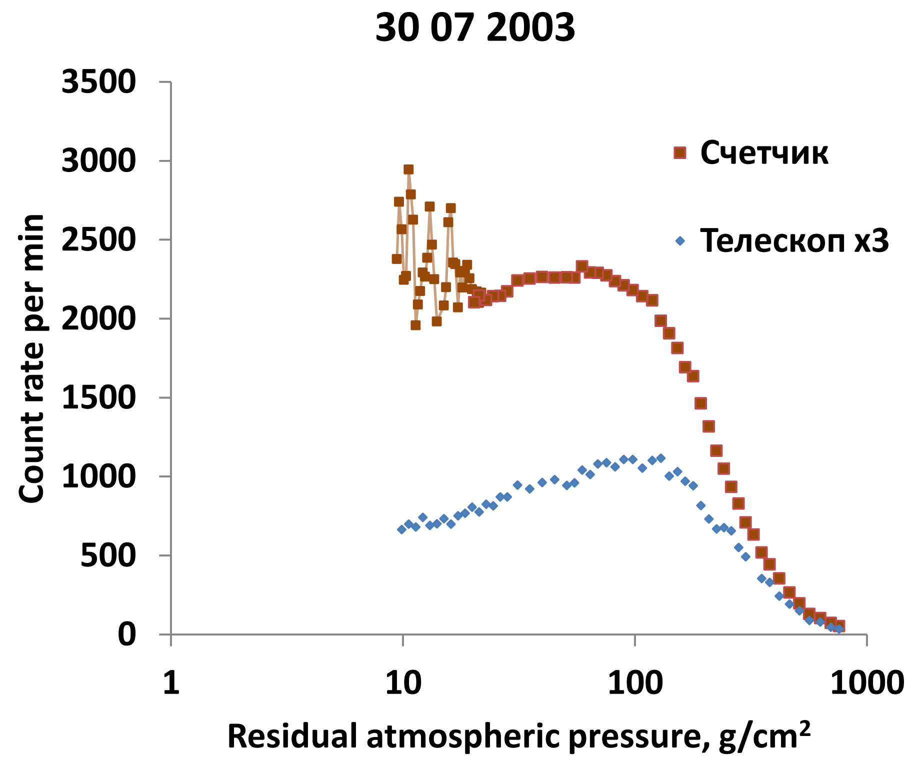

Examples of electron precipitation observations at Apatity, Murmansk region. No effect in the telescope records and strong fluctuations are indicative of EEP.

Compilation of EEP observations is published as

Makhmutov V.S., Bazilevskaya G.A., Stozhkov Yu.I., Svirzhevskaya A.K., Svirzhevsky N.S. Catalogue of electron precipitation events as observed in the long-duration cosmic ray balloon experiment. J. Atmos. Solar Terr. Phys., 2016, v. 149, 258-276. http://dx.doi.org/10.1016/j.jastp.2015.12.006i
Also: http://sites.lebedev.ru/DNS_FIAN/show.php?page_id=479

Station	Geograph. Coordinates	Rc(GV) / McIlwain L	Start time of balloon launch (UT)	Period of measurements	Number of balloon launches	Number of EPEs recorded
Olenya, Murmansk region	68°57′N, 33°03′E	0.6/5.2-5.8	08	07/1957-2002	~40000	524
Apatity, Murmansk region	67°33′N, 33°20′E	0.6/5.2-5.3	15	2002-present time		
Mirny, Antarctica	66°34′S, 92°55′E	0.03	09	03/1963–present time	16700	10
Norilsk	69°00′N, 88°00′E	0.6	08	11/1974–06/1982	760	10
Tixie Bay	71°36′N, 128°54′E	0.5	08	02/1978–10/1987	1190	17

The Catalog is a subject of revisiting and constant work aimed at correction and improvement.

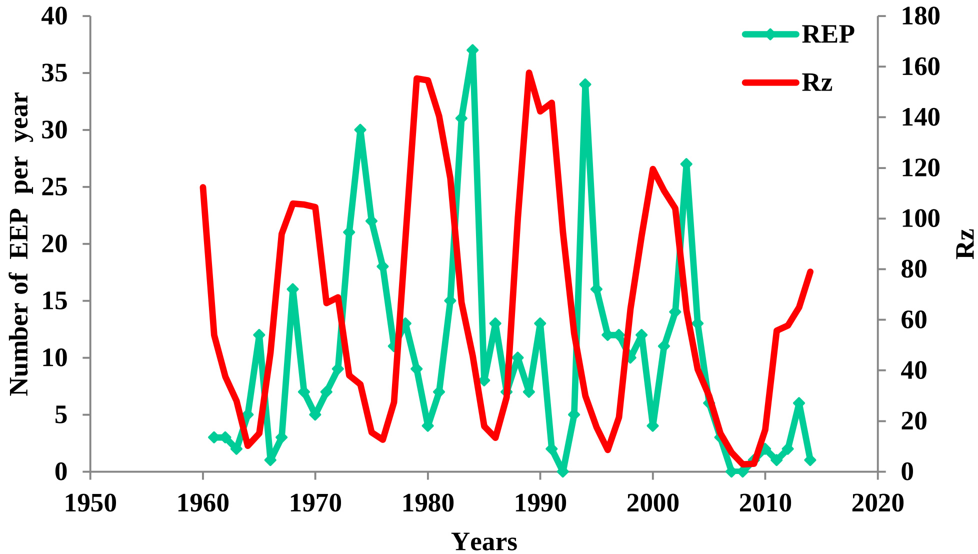

Events of energetic electron precipitation are most frequent at the decay phase of the 11-year solar cycle.

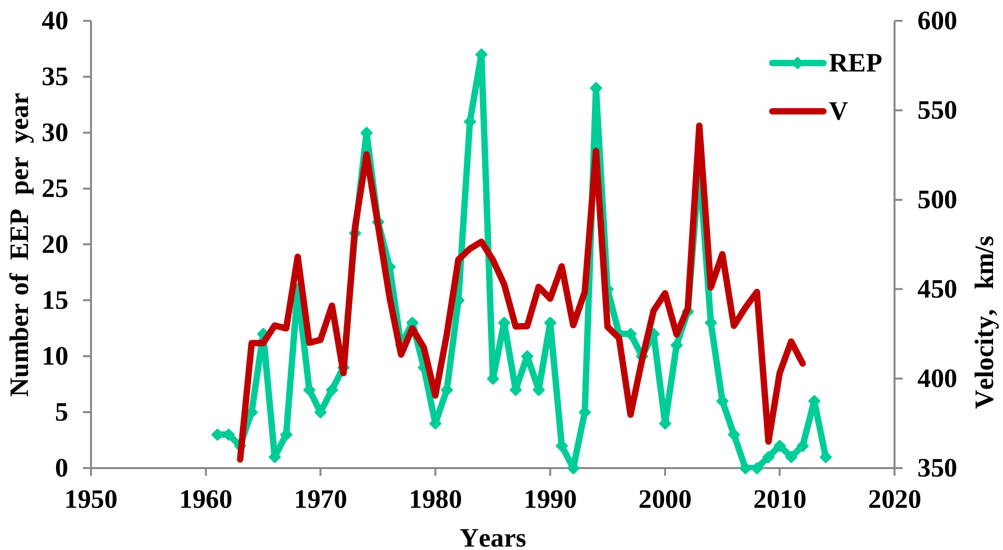

The precipitation rate correlates with the solar wind velocity.
Precipitation correlates with the high speed solar wind streams.

Recent view on the processes leading to magnetospheric electron precipitation

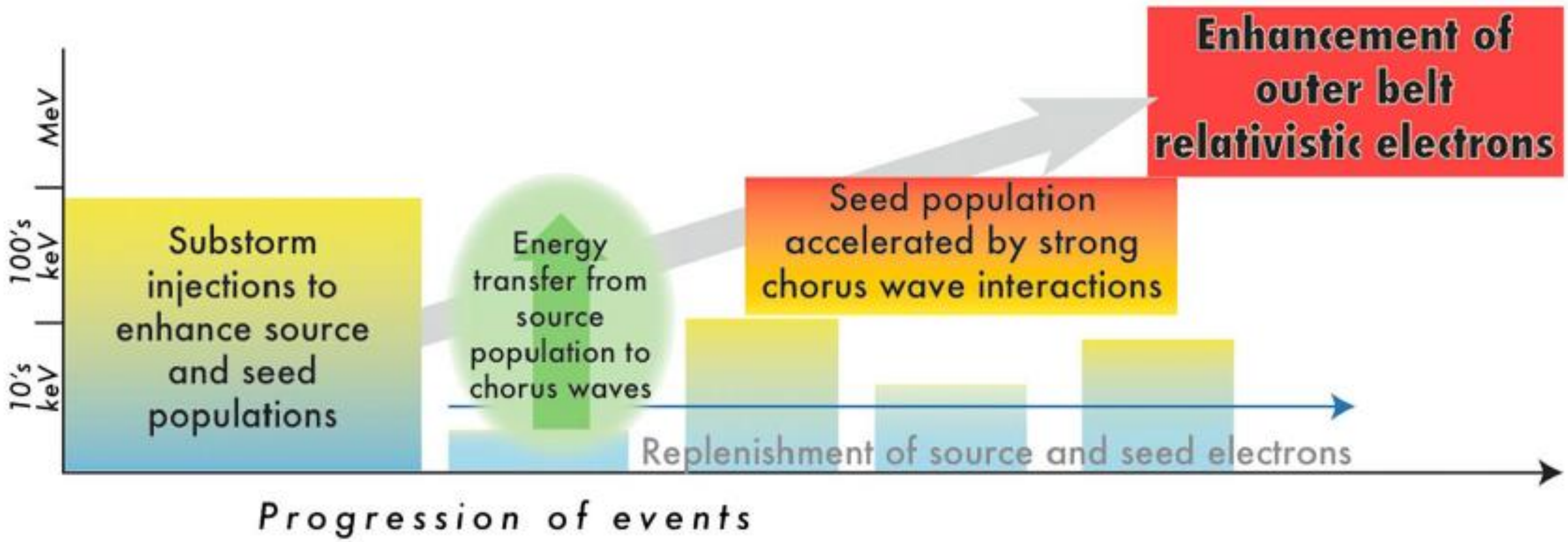

Figure 1. Schematic of the ideal setup and sequence for strong enhancement of outer belt electrons >1 MeV.

Jaynes et al., 2015

Recent view on the processes leading to magnetospheric electron precipitation

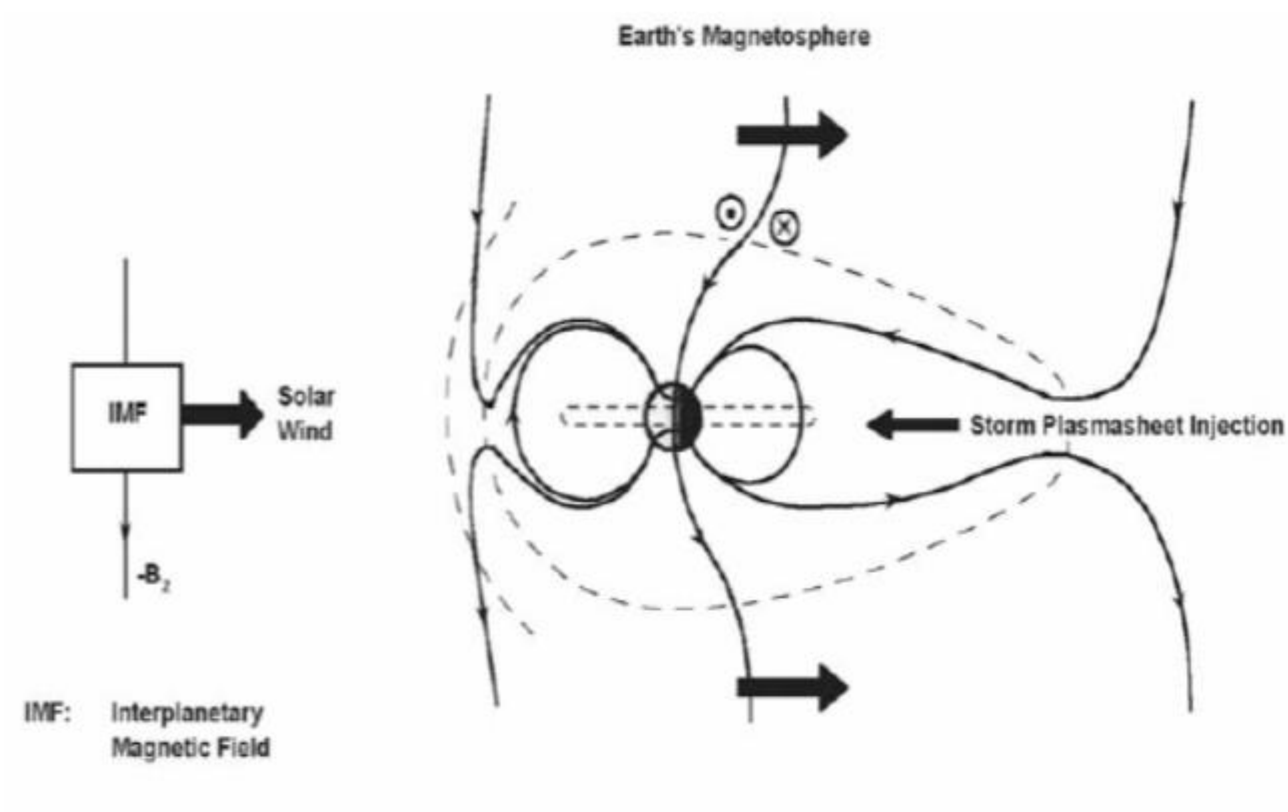

1. Energy input from space to magnetosphere under southward B condition (magnetic reconnection)

Importance of the Bz direction

The product of the solar wind radial flow speed and the southward magnetic field strength (V·Bz) is indicative of the solar wind energy injected into the terrestrial system [Owens et al, 2005; Gopalswamy et al., 2015 and references therein)].

The dusk to dawn electric field (E_Y in GSE coordinates, the product of the solar wind radial flow speed and the southward magnetic field strength) plays a major role in the modulation of magnetic reconnection (interconnection!! Lemair) at the dayside magnetopause and hence controls the rate at which solar wind energy can be injected into the terrestrial system [Dungey, 1961]

Recent view on the processes leading to magnetospheric electron precipitation

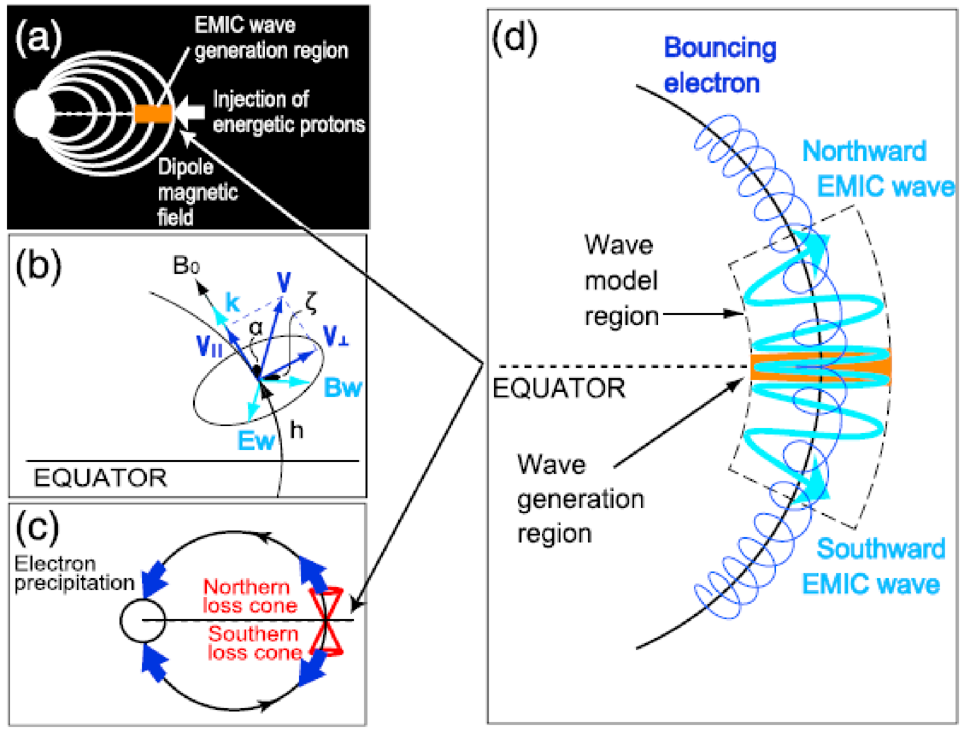

Figure 1. A schematic illustration of the generation of EMIC-triggered emissions and interaction with relativistic electrons. (a) EMIC wave generation around the equator by injected energetic protons in a dipole magnetic field. (b) Vector components of an EMIC wave and velocity components of a test electron. (c) Electron precipitation due to scattering induced by EMIC waves. (d) Mirror motion of relativistic electrons interacting with the wave packets repeatedly.

Kubota et al., 2015

El. 2 MeV
Cyclotron frequency
n100 –n1000 Hz
(VLF, ELF)
T bounce 1 s,
Tdrift 9 min

Proton 2 MeV
Cyclotron frequency
nHz (<ULF)
T bounce 11 sec,.,
Tdrift 9 min

2. Wave generation and particle acceleration

3. Particle scattering and precipitation

A schematic illustration of radiation belt structures and processes

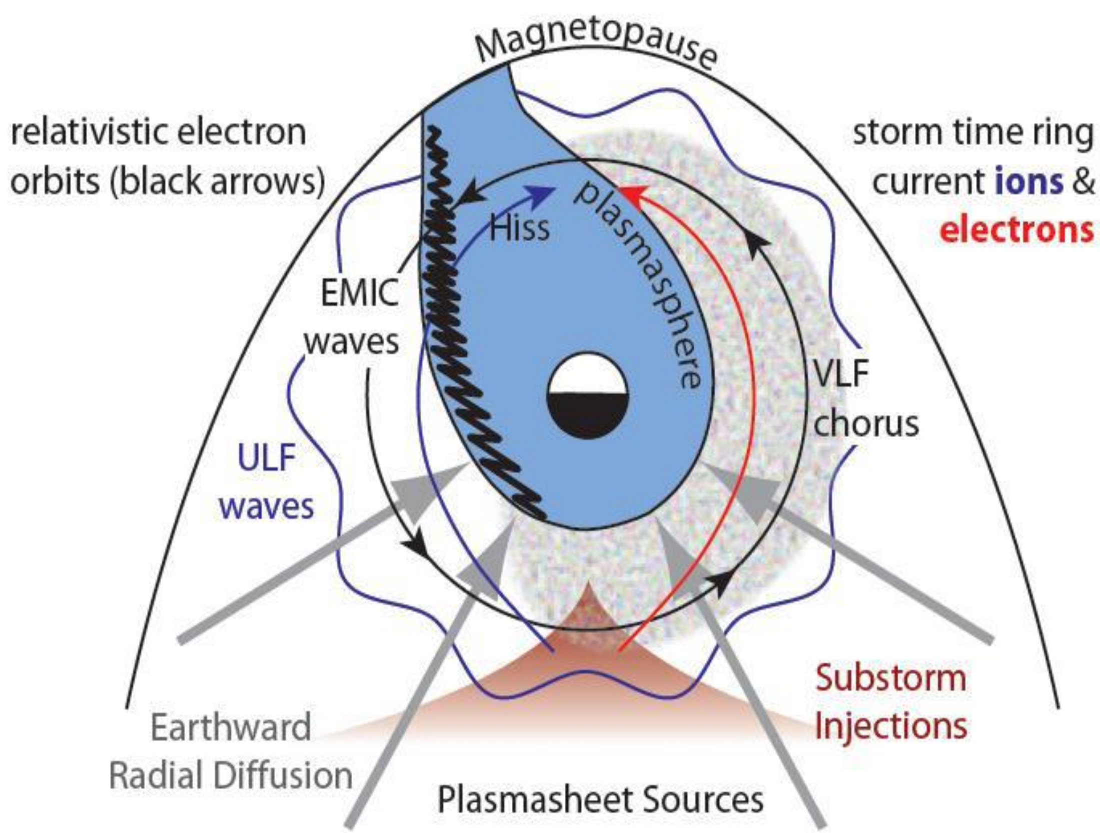

Various wave modes are generated predominantly in different regions of the magnetosphere: whistler-mode chorus outside of the plasmasphere, electromagnetic ion cyclotron waves (EMIC) on or around the plasmapause, and whistler mode hiss inside the plasmasphere [Reeves et al., 2009].

Waves

Hiss 3-5 kHz
Chorus 5-7 kHz
ULF: 3-30 Hz
EMIC 0.1-5 Hz

El. 2 MeV
Cyclotron frequency n100 –n1000 Hz (VLF, ELF)
Ro=34 km (equator)
T bounce 1 s,., Tdrift 9 min

Proton 2 MeV
Cyclotron frequency nHz (<ULF)
Ro=1400 km (equator)
T bounce 11 sec,., Tdrift 9 min

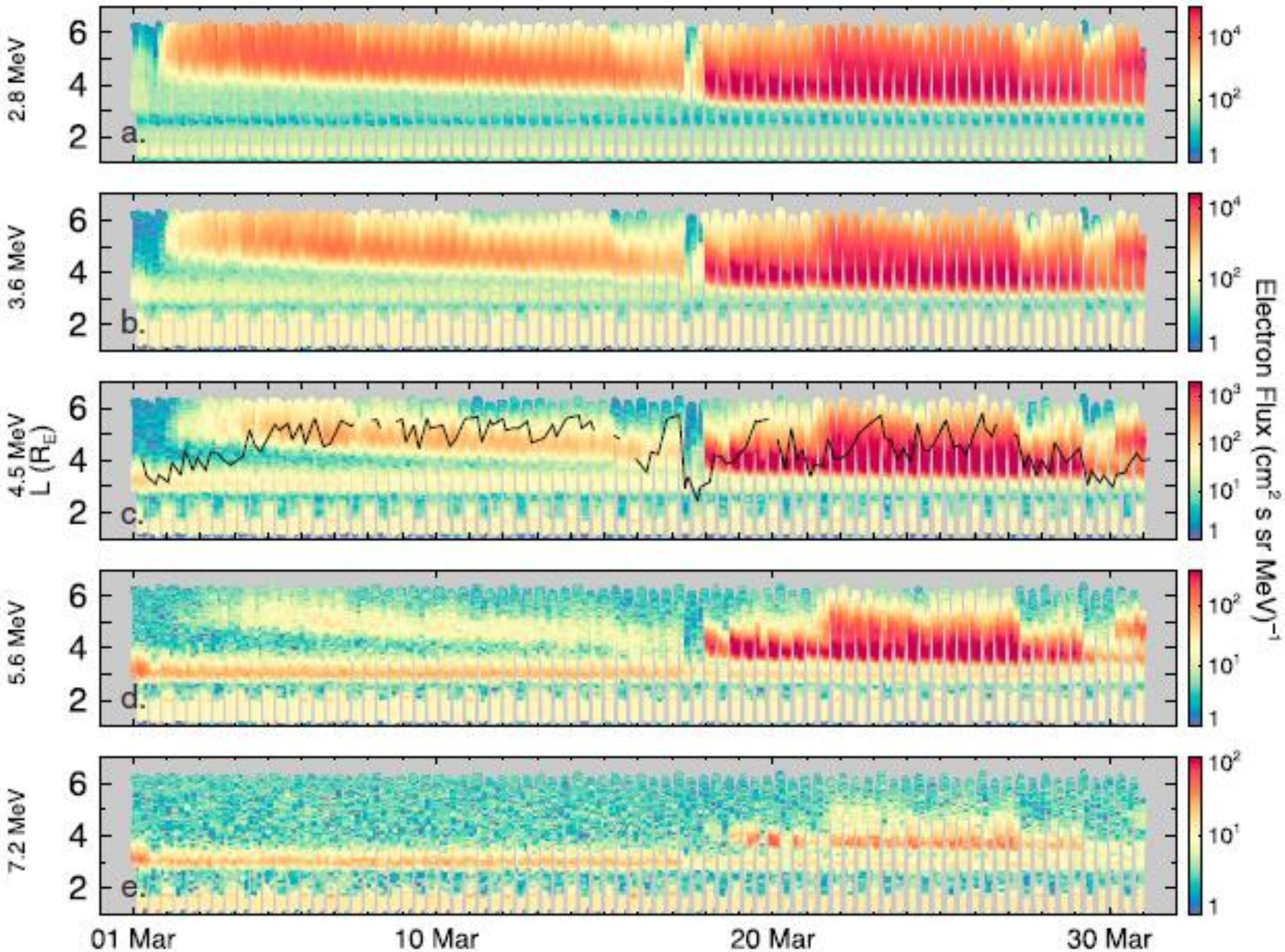

Figure 2. Details of multi-MeV electron flux variations (see Figure 1) for the month of March 2013. The black trace on Figure 2c represents the plasmapause location derived from EFW spacecraft density measurements.

Baker et al., 2014

Importance of the plasmapause location

Over time periods of weeks to months the plasmapause location was a good indication of the inner edge of the outer radiation belt [Li et al., 2006]. This relationship breaks down on shorter time periods. This is clearest for events where the plasmapause moves inward, allowing chorus to accelerate electrons to higher energies at comparatively low L shells, and then outward, leaving this high-energy population inside the plasmapause. A particularly dramatic example of this is the recent reports of the "third radiation belt" observed by the Van Allen Probes [*Baker et al.*, 2013] [Whittaker, 2014]

$L\mathrm{pp}(t) = -0.7430 \ln(\max(t-1, t\ Ap)) + 6.5257$ [Kamp et al., 2016]

Max(t-1,t Ap) indicates the maximum value of *Ap* of the day of the current and the previous day.

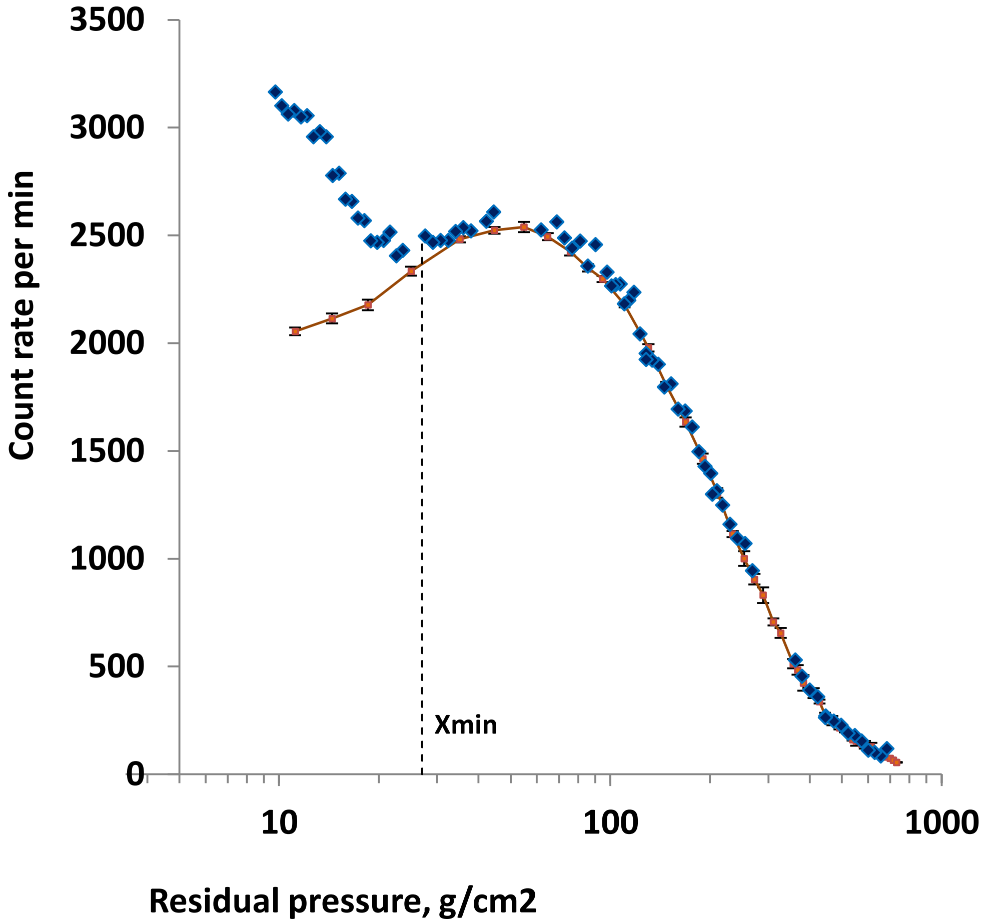

Xmin –height (pressure) of start of EPE observation.

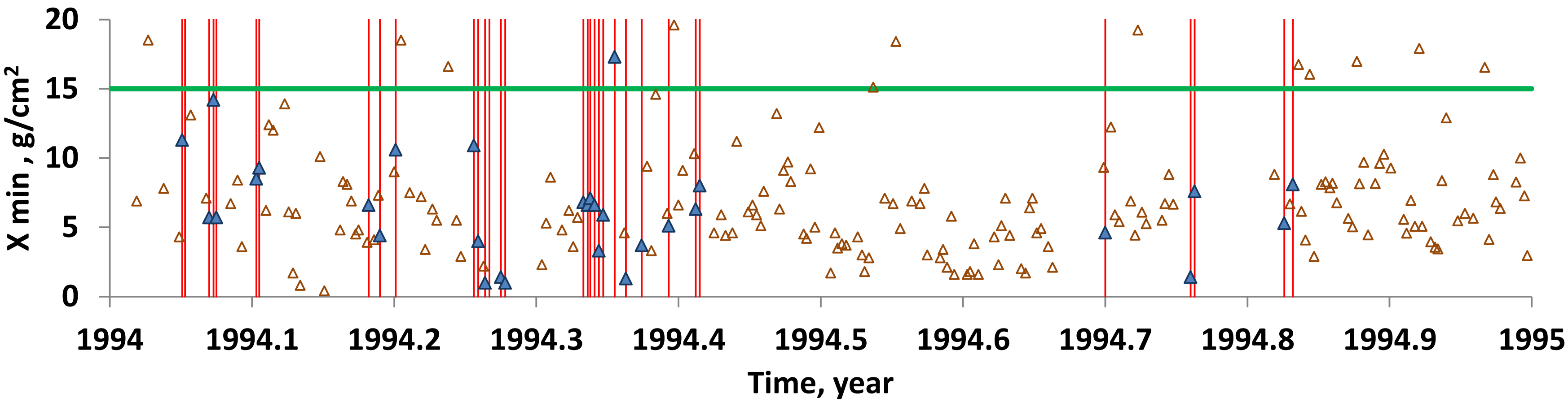

Blue pluses – Xmin at EEP
Open pluses – all launches
Red bars – time of EEP

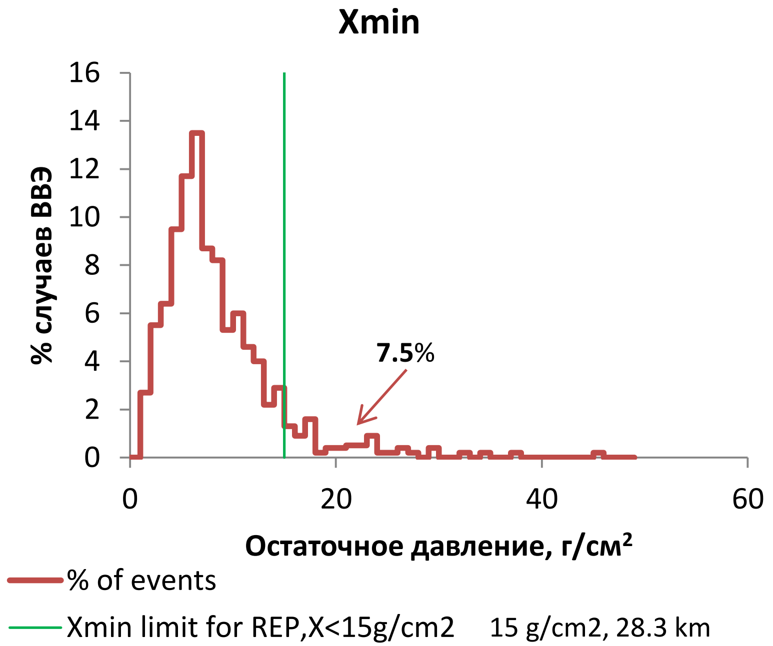

Xmin – minimal residual pressure in a balloon flight (ceiling altitude)

Высыпания в 1994 г. → Обоснование перехода к полугодовым данным

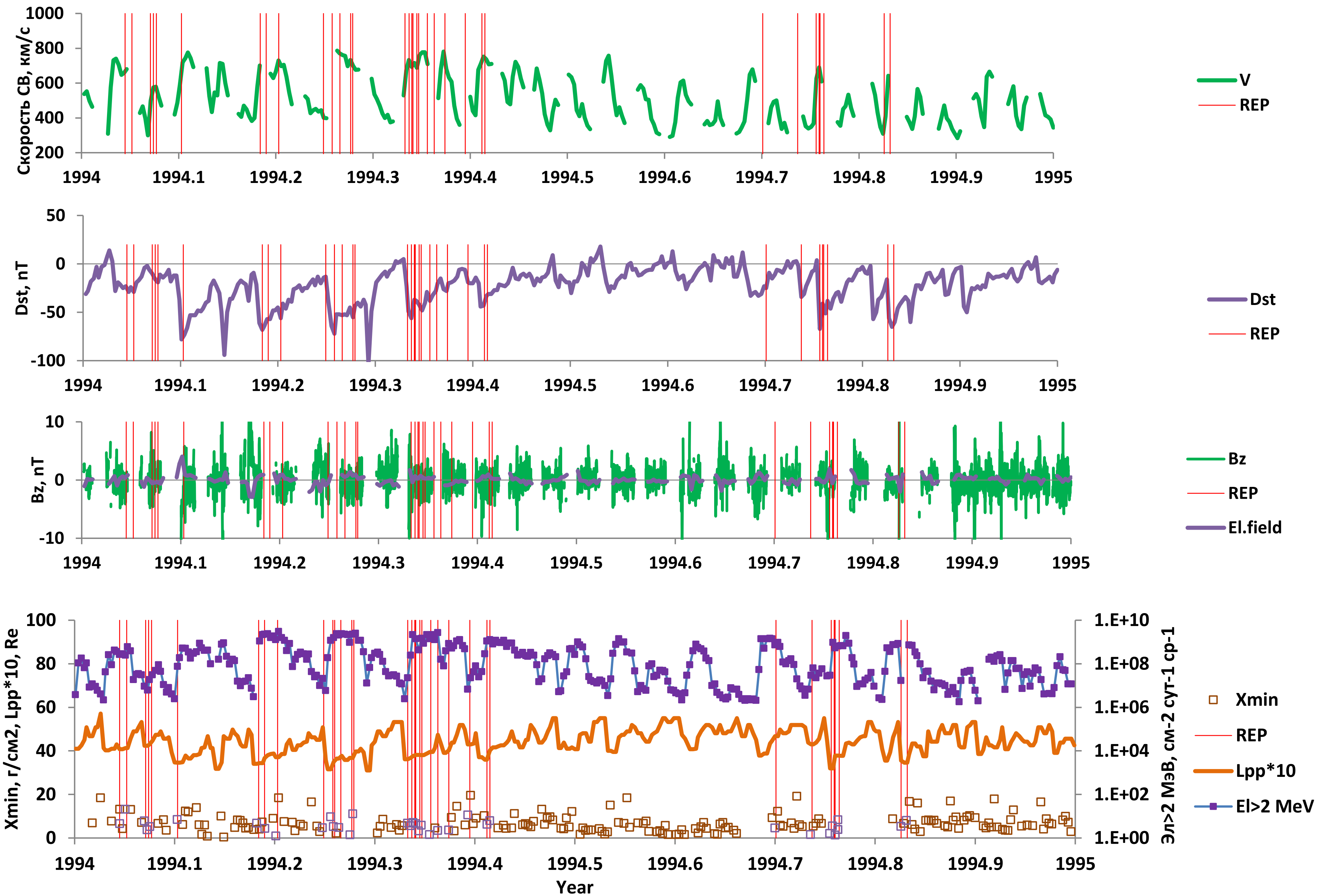

MEPHI, Wednesday 21 June 2017

Seasonal variation

This modulation can be explained by an increase in the average energy injected into the magnetosphere for each storm during the equinoctial months.
Some process makes magnetic reconnection less efficient when the Earth's dipole axisis tilted along the Earth–Sun line (the Russell–McPherron effect).
Quantitive analysis shows that seasonal variation is not fully explained by the R-McPh effect although it makes the major contribution.

Russel and McPherron , 1973,
McPherron et al., 2009, 2013

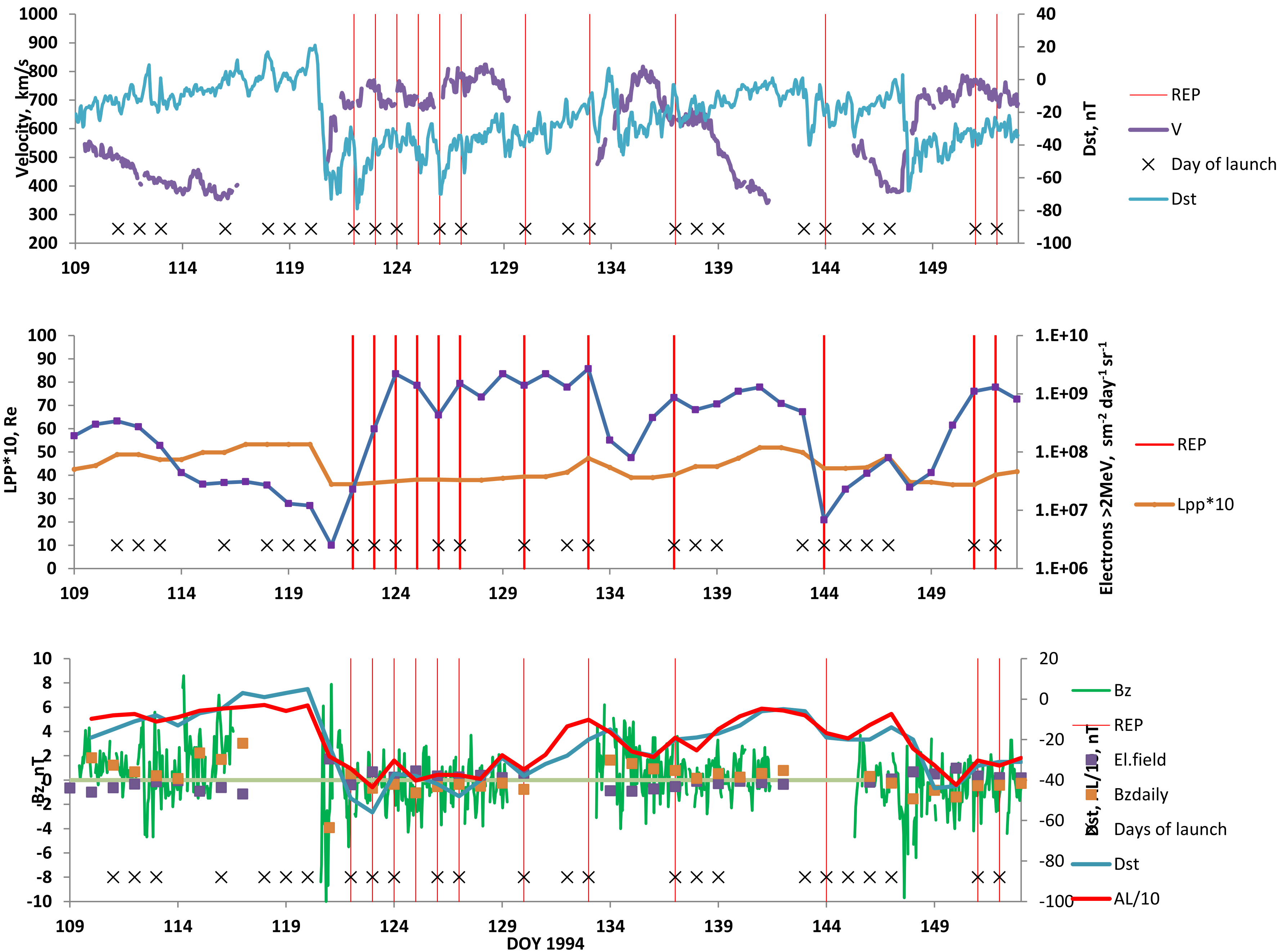

Velocity, km/s
Dst, nT
REP
V
Day of launch
Dst
LPP*10, Re
Electrons >2MeV, $sm^{-2}\ day^{-1}\ sr^{-1}$
REP
Lpp*10
-Bz, nT
Dst, AL/10, nT
Bz
REP
El.field
Bzdaily
Days of launch
Dst
AL/10
DOY 1994

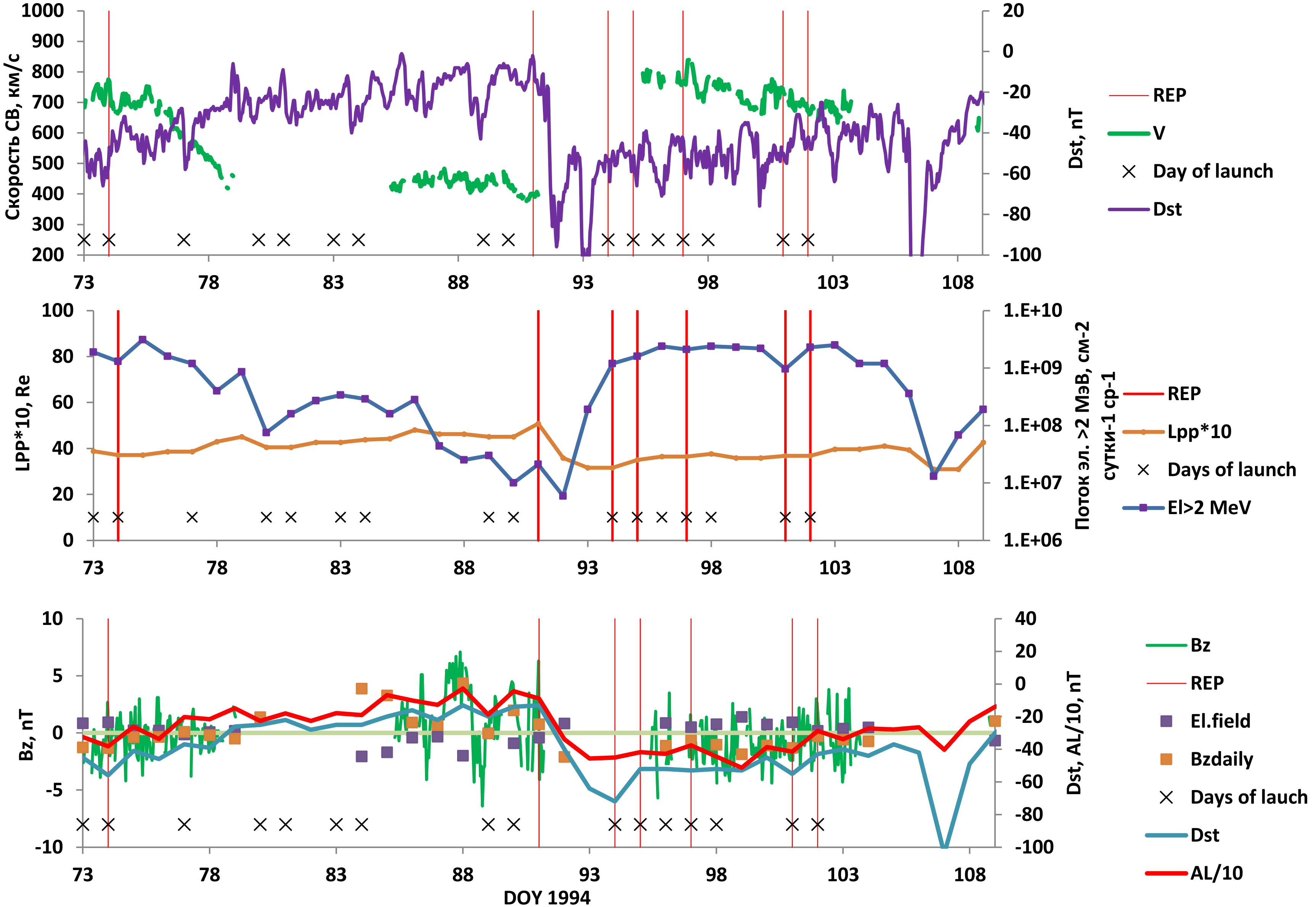
1000
900
800
700
600
500
400
300
200
Скорость СВ, км/с
20
0
-20
-40
-60
-80
-100
Dst, nT
REP
V
Day of launch
Dst
73
78
83
88
93
98
103
108
100
80
60
40
20
0
LPP*10, Re
1.E+10
1.E+09
1.E+08
1.E+07
1.E+06
Поток эл. >2 МэВ, см-2 сутки-1 ср-1
REP
Lpp*10
Days of launch
El>2 MeV
10
5
0
-5
-10
Bz, nT
40
20
0
-20
-40
-60
-80
-100
Dst, AL/10, nT
Bz
REP
El.field
Bzdaily
Days of lauch
Dst
AL/10
DOY 1994

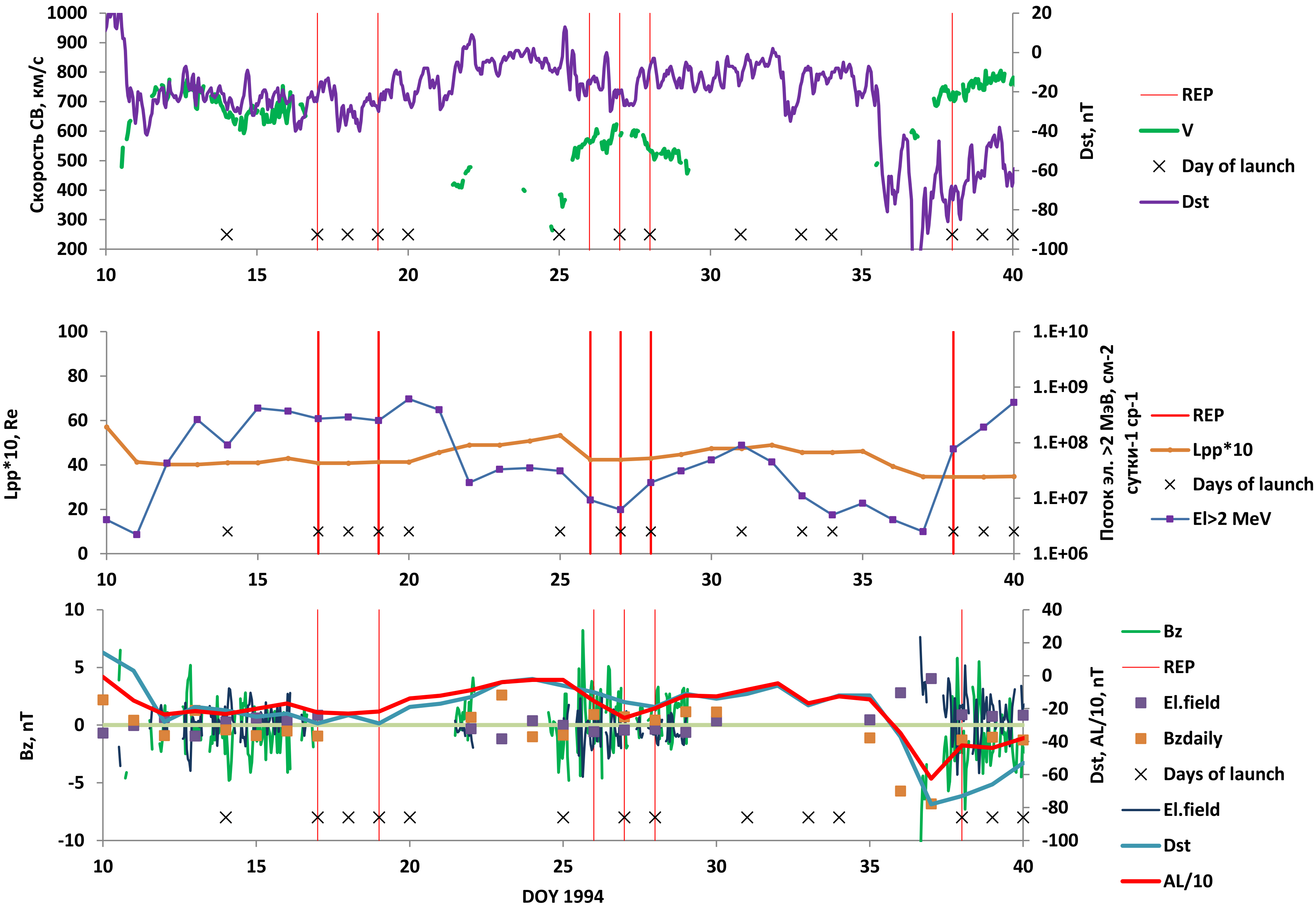
Скорость СВ, км/с
Dst, nT
REP
V
Day of launch
Dst
Lpp*10, Re
Поток эл. >2 МэВ, см-2 сутки-1 ср-1
REP
Lpp*10
Days of launch
El>2 MeV
Bz, nT
Dst, AL/10, nT
Bz
REP
El.field
Bzdaily
Days of launch
El.field
Dst
AL/10
DOY 1994

Human Radio Transmissions Create Barrier to "Killer Electrons"
An interaction between radio waves and the Van Allen radiation belts creates a bubble around the Earth that high-energy electrons can't penetrate.

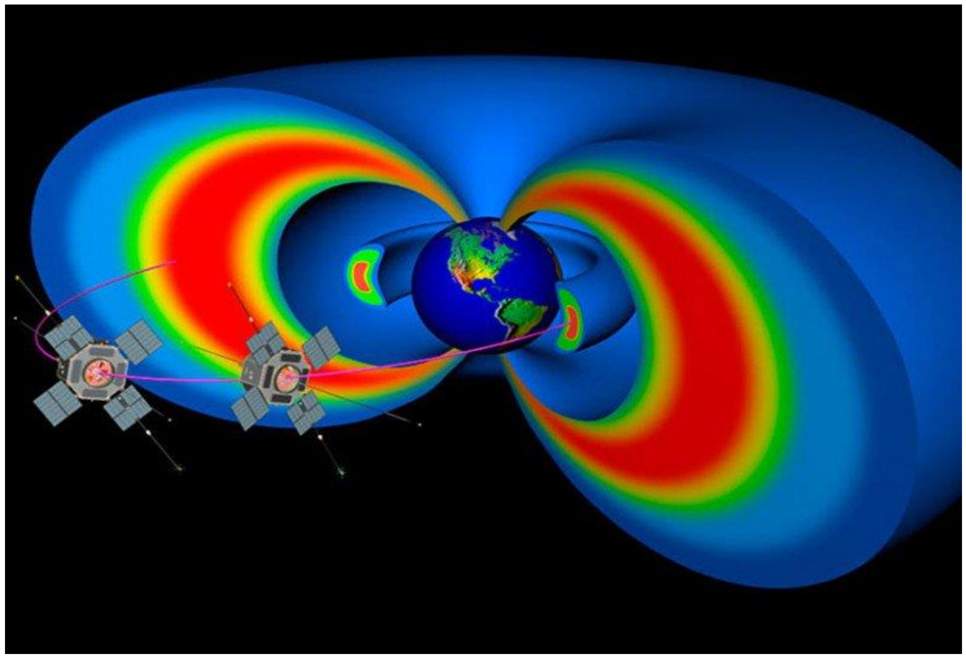

Scientists discovered that very low frequency radio transmissions from Earth may help to create an “impenetrable barrier” at the inner edge of the outer belt that keeps the belt’s “killer electrons” away from Earth. Credit: NASA
Wendel, J. (2015), Human radio transmissions create barrier to “killer electrons”, Eos, 96, doi:10.1029/2015EO041853. Published on 16 December 2015.

Conclusion

Episodes of EEP events in March, May, and September 1994 are in agreement with expected behavior initiated by

- **arrival of a high speed solar wind stream:**
- **a geomagnetic disturbance (Dst),**
- **southward Bz during rather a long time period,**
- **moving of the plasmapause location,**
- **high fluences of relativistic electrons in the outer radiation belt.**

Calm in EEP in summer of 1994 is well-known although not fully explained effect.

Some EEP events in January 1994 do not have clear connection with a high speed solar wind stream. Could they be caused by a VLF transmitters?

Thank you!